RSC Advances

PAPER

View Article Online
View Journal | View Issue

Cite this: *RSC Adv.*, 2024, **14**, 5514

Tandem manganese catalysis for the chemo-, regio-, and stereoselective hydroboration of terminal alkynes: *in situ* precatalyst activation as a key to enhanced chemoselectivity†

Victor Duran Arroyo and Rebeca Arevalo *

Received 22nd December 2023
Accepted 5th February 2024

DOI: 10.1039/d3ra08747f

rsc.li/rsc-advances

The manganese(II) complex [Mn(^{iPr}PNP)Cl$_2$] (^{iPr}PNP = 2,6-bis(diisopropylphosphinomethyl)pyridine) was found to catalyze the stereo- and regioselective hydroboration of terminal alkynes employing HBPin (pinacolborane). In the absence of *in situ* activators, mixtures of alkynylboronate and *E*-alkenylboronate esters were formed, whereas when NaHBEt$_3$ was employed as the *in situ* activator, *E*-alkenylboronate esters were exclusively accessed. Mechanistic studies revealed a tandem C–H borylation/semihydrogenation pathway accounting for the formation of the products. Stoichiometric reactions hint toward reaction of a Mn–H active species with the terminal alkyne as the catalyst entry pathway to the cycle, whereas reaction with HBPin led to catalyst deactivation.

Introduction

The discovery of chemoselective catalysts for the functionalization of small molecules is key to access versatile synthons with applications in fine chemistry. The functionalization of alkynes with boronate esters (HB(OR)$_2$) is a widely-used transformation, providing access to synthetically valuable alkynyl-, alkenyl- or alkyl-boronate esters.[1] However, when the alkyne is terminal, chemoselectivity issues arise due to the competition of the functionalization of the triple and of the C(sp)–H bonds, and the control of the chemoselectivity of the reaction employing a catalyst is key. In transition metal-catalyzed reactions of terminal alkynes with boronate esters, the preferred reactivity, either hydroboration[2] or C–H borylation,[3] is determined by the identity of the metal complex, which dictates whether C–H activation or alkyne insertion steps are preferred. To avoid this competition, some catalysts have been reported to be efficient only for internal alkynes,[4] and there are few insights into the keys leading to chemoselective hydroboration of terminal alkynes,[2c,d] including how the other components of the catalytic system (such as *in situ* activators, solvent identity or temperature) impact the chemoselectivity.[2d]

Manganese catalysis is a rising field, with Mn(I) catalysts containing CO ligands being well-established, particularly for reduction processes.[5] In contrast, low-oxidation state (0, +I or +II) Mn complexes lacking CO ligands have been comparatively less explored for small molecule functionalization.[6] We have recently reported that when the manganese complex [Mn(SiNSi)Cl$_2$][6a] (**Mn1**) was employed as precatalyst for the functionalization of terminal alkynes with HBPin, alkynylboronate esters

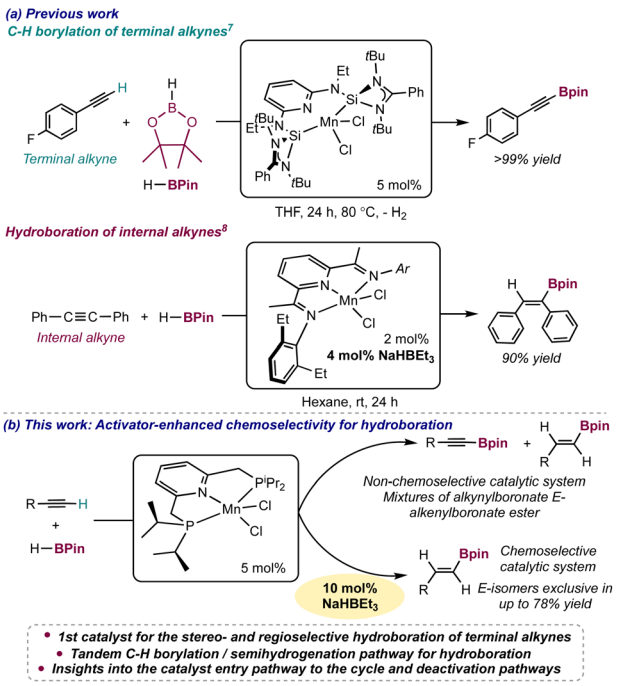

Scheme 1 (a) Manganese-catalyzed dehydrogenative borylation of terminal alkynes (top) and hydroboration of internal alkynes (bottom) with two different Mn complexes; (b) this work: stereo- and regioselective hydroboration of terminal alkynes.

Department of Chemistry and Biochemistry, University of California, 5200 North Lake Road, 95343, Merced, California, USA. E-mail: rebecaarevalo@ucmerced.edu

† Electronic supplementary information (ESI) available: Complete experimental details, characterization data, NMR spectroscopic data. See DOI: https://doi.org/10.1039/d3ra08747f

were exclusively formed by C–H borylation (Scheme 1a, top).[7] However, this precatalyst was found inefficient for the functionalization of either internal or terminal alkynes when it was *in situ* activated with $NaHBEt_3$. In contrast, Rueping and coworkers reported that *in situ* activation with $NaHBEt_3$ triggered the catalytic activity of the $[Mn(^{Et}PDI)Cl_2]$ complex in the hydroboration of symmetrical internal alkynes to yield alkenylboronate esters from the *syn* addition of HBPin (Scheme 1a, bottom).[8] However, the substrate scope was limited to symmetric internal alkynes, where competition of C(sp)–H activation was not a concern. Whereas Earth-abundant transition metal catalysts, mainly of Fe and Co,[2b–d,f–o] for the hydroboration of terminal alkynes are known, most of them being *Z*-stereoselective, a manganese catalyst for this transformation has not been described. Due to manganese being the third most abundant transition-metal in the Earth crust, a manganese catalyst for this process would contribute to the development of sustainable processes in synthetic chemistry. The main challenge to address to discover this catalyst is to understand which components of the catalytic system play a role in controlling the chemo-, stereo- and regioselectivity of the reaction for the functionalization of terminal alkynes.

Interested in elucidating the role that the ligand plays on the chemoselectivity of the manganese-catalyzed reaction between a terminal alkyne and HBPin, we hypothesized that a Mn complex containing a less electron-donating and sterically hindered pincer ligand than the SiNSi[9] in **Mn1**, may render access to a catalyst capable of insertion steps affording alkenylboronate esters. In this work we report that the Mn(II) complex, $[Mn(^{iPr}PNP)Cl_2]$, is the first catalyst for the hydroboration of unactivated terminal alkynes showing an excellent stereo- and regio-selectivity for the *E*-alkene upon *in situ* activation with $NaHBEt_3$. The role of $NaHBEt_3$ as activator is key to enhance the chemoselectivity of the catalyst for hydroboration. Insights into the reaction pathway as well as on the precatalyst entry to the cycle and deactivation pathways are provided.

Results and discussion

Catalytic competency of $[Mn(^{iPr}PNP)Cl_2]$ for the functionalization of terminal alkynes with HBPin

Our research commenced with the synthesis of the manganese precatalyst $[Mn(^{iPr}PNP)Cl_2]$[10] (**Mn2**, ^{iPr}PNP = 2,6-bis(diisopropylphosphinomethyl)pyridine) and the assessment of its efficiency for the functionalization of phenylacetylene (**1**) with HBPin (Pin = pinacolate) in the absence of strong hydride or alkyl sources as *in situ* activators. The initial conditions employed for the reaction were those identified as optimal in our lab for the C–H borylation of terminal alkynes catalyzed by $[Mn(SiNSi)Cl_2]$ (**Mn1**)[7] (5 mol% catalyst loading, 2.5 equiv. HBPin, 80 °C, 24 h, 0.5 M solution in THF). Under these conditions, **Mn2** led to a low conversion of the starting material (23%) affording the *E*-alkenylboronate ester **1b** as the major product in a 14% yield, with the alkynylboronate ester **1a** formed in <5% yield (crude yields and conversion determined by GC). A mixture of the alkynyl (15% yield) and the *E*-alkenylboronate ester (7% yield) was obtained for 4-fluorophenylacetylene with the reaction also proceeding to low conversion (24%, see page S5 in the ESI†). However, when 2-fluoro- or 3-fluorophenylacetylene were employed as substrates, the reactions proceeded to 51% and 52% conversions respectively affording the corresponding alkynylboronate esters exclusively (45% and 19% yields respectively, see page S5 in the ESI†). These results suggest that **Mn2** is less efficient than **Mn1** for the functionalization of terminal alkynes with HBPin and lacks chemoselectivity, as the identity of the substrate was capable of determining whether hydroboration or C–H borylation was preferred. Employing the Mn(II) dihalide complexes containing a ^{tBu}PNP (2,6-bis(di-*tert*-butylphosphinomethyl) pyridine, **Mn3**) or a ^{Et}PDI ligand (^{Et}PDI = (2,6-diethylphenyl) pyridyldiimine, **Mn4**,[8] see entries 3 and 4 in Scheme 2a) as precatalysts, resulted in low conversion of the starting material with formation of the *E*-alkenylboronate ester as the major

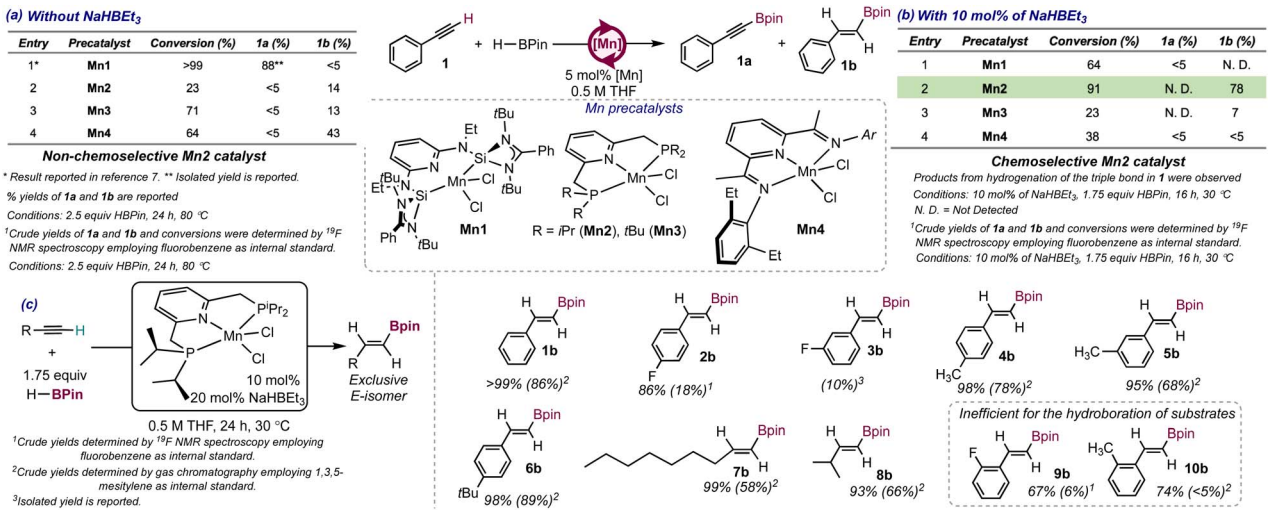

Scheme 2 Catalyst screening for the functionalization of phenylacetylene with HBPin (a) without and (b) with $NaHBEt_3$ as *in situ* activator and (c) substrate scope for the hydroboration of terminal alkynes employing **Mn2**/$NaHBEt_3$ as precatalyst.

product, although in low to moderate yields (13% for **Mn3** and 43% for **Mn4**). It is worth noting that all the precatalysts employed (**Mn2**-**Mn4**) were chemoselective for hydroboration when phenylacetylene was employed as the substrate, suggesting that the stronger-electron donating and sterically demanding SiNSi ligand in **Mn1** is key to favor C–H borylation over hydroboration.

Aiming to understand the factors that contributed to the loss of the chemoselectivity, the functionalization of 4-fluorophenylacetylelene (**2**) with HBPin catalyzed by **Mn2** was monitored for 4 hours by ^{1}H, ^{19}F, ^{11}B and ^{31}P NMR spectroscopy in THF-d_8 at 80 °C in a J. Young NMR tube where the headspace was evacuated (see pages S15–S19 in the ESI†). The results support that both products, the alkynyl- (**2a**, at −108.4 ppm in the ^{19}F NMR spectrum) and the *E*-alkenylboronate (**2b**, at −111.9 ppm in the ^{19}F NMR spectrum) esters were formed in a 0.8 : 1 **2a** : **2b** ratio after 1 h (determined by integration of the ^{19}F NMR spectrum). In contrast, when **Mn1** was employed as precatalyst, product **2b** was only formed at high substrate conversion,[7] again highlighting the key role of the SiNSi ligand in the chemoselectivity for C–H borylation. The **2a** : **2b** ratio changed over the course of 4 hours (1.4 : 1 after 2 h, 2.3 : 1 after 3 h and 3.4 : 1 after 4 h), hinting a faster increase in the amount of alkynylboronate ester than that of *E*-alkenylboronate ester, and suggesting two independent catalytic cycles operative in solution, one for C–H borylation and one for hydroboration. Further supporting this hypothesis, the ^{31}P NMR spectra showed two signals at 38.0 and 38.5 ppm, consistent with the presence of two diamagnetic catalyst-resting states, one for each of the cycles operative (see Fig. S5 in the ESI†).

Hydroboration of terminal alkynes with HBPin catalyzed by [Mn(^{iPr}PNP)Cl$_2$] in the presence of NaHBEt$_3$ as *in situ* activator

Aiming to determine the impact that the presence of a strong hydride or alkyl source as *in situ* activator had on the chemoselectivity of the catalytic system, the efficiency of **Mn2** for the functionalization of **1** with HBPin was assessed in the presence of strong hydride and alkyl sources. Employing 10 mol% of RLi (R = Me, Ph) or KO*t*Bu as *in situ* activators of 5 mol% of **Mn2** resulted in poor conversion of **1** and yield of the *E*-alkenylboronate ester **1b** (see Table S1 in the ESI†). In contrast, when 10 mol% of NaHBEt$_3$ were employed as the activator, full conversion of the starting material was observed, with **1b** being formed as the major product in a 78% yield (see Scheme 2b, entry 2 in table). The *E*-isomer was exclusively obtained, and neither the *Z* isomer, α-alkenylboronate esters nor product **1a** were detected by GC in the reaction crude, supporting **Mn2**/NaHBEt$_3$ as the first stereo-, regio- and chemoselective catalytic system for the hydroboration of **1**. Styrene was detected in <5% yield in the crude reaction mixture by GC, as well as trace amounts of 1,2,4 and 1,3,5-triphenylbenzene from alkyne cyclotrimerization.[11]

The presence of styrene in the reaction medium can be attributed to the semihydrogenation of **1** catalyzed by **Mn2**/NaHBEt$_3$ and is consistent with the report of **Mn2** as an efficient catalyst for the *Z*-selective semihydrogenation of internal and terminal alkynes employing NH_3BH_3 as the H_2 source.[10]

Whereas the use of NaHBEt$_3$ as *in situ* activator in the reaction of **1** with HBPin catalyzed by **Mn1** led to a mixture of unidentified products (see Scheme 2b, entry 1 in table), the results presented above support that **Mn2** was capable of generating an active species by reaction of NaHBEt$_3$ that catalyzed the hydroboration of **1**. The presence of NaHBEt$_3$ as the activator increased the catalyst efficiency but, more importantly, was key to drive the chemoselectivity of the reaction toward hydroboration. Employing [Mn(^{tBu}PNP)Cl$_2$] (**Mn3**) as the precatalyst, containing *t*Bu groups at the P-donors, resulted in a lower conversion of the starting material (23%) and the formation of **1b** in low yield (7%) (Scheme 2b, entry 3 in table). Even though **Mn4** has been previously reported as an efficient catalyst for the hydroboration of internal alkynes,[8] it showed poor catalytic activity for the hydroboration of terminal alkynes under the conditions in Scheme 2b (see entry 4 in table).

Control experiments for the reaction of **1** and HBPin in THF at 30 °C for 24 h were run (a) in the presence of 10 mol% of NaHBEt$_3$, (b) in the presence of 5 mol% of MnCl$_2$ and 10 mol% of NaHBEt$_3$, (c) in the presence of 5 mol% of ^{iPr}PNP and 10 mol% of NaHBEt$_3$ and (d) without any added species (see pages S10–S12 in the ESI†). In all cases, the reactions proceeded to <35% conversion of the starting material yielding a mixture of products that did not include **1b** except in (c) and (d) where **1b** was formed in <5% yield (determined by GC). These results support the need of all the reagents to access **1b** in a synthetically useful yield and rule out trace borane as the species responsible for the catalytic activity (experiment (a)).[12]

Encouraged by the chemoselectivity shown by the **Mn2**/NaHBEt$_3$ system for the reaction of **1** with HBPin, we set out to investigate the factors that impacted the yield of the product. The efficiency of other borylating agents, mainly HBDan and B_2Pin_2 for the functionalization of **1** was assessed (see Table S2 in the ESI†). In both cases, the yields for **1b** were lower than when HBPin was employed (<5% for HBDan and <5% for B_2Pin_2). Employing 5 mol% of MnCl$_2$, 5 mol% of ^{iPr}PNP and 10 mol% of NaHBEt$_3$ as the precatalyst instead of *in situ* activated **Mn2**, led to a catalytic activity comparable to that of **Mn2**/NaHBEt$_3$ (74% yield for **1b**), suggesting that the active species can be *in situ* generated from the previous mixture. In contrast, when MnBr$_2$, Mn(OAc)$_2$ or Mn(OTf)$_2$ were employed as the Mn source, the yield of **1b** decreased significantly (18% yield of **1b** for MnBr$_2$ and <5% yield for Mn(OAc)$_2$ and Mn(OTf)$_2$, see Table S3 in the ESI†), highlighting the relevance of the Mn source in the formation of the active species. The order of addition of the components in the catalytic reaction also impacted the yield of **1b** (see Table S4 in the ESI†). When (a) NaHBEt$_3$ was added to a mixture of **Mn2** and **1** followed by the addition of HBPin, the yield of **1b** decreased to 44%, whereas when (b) NaHBEt$_3$ was added to a mixture of **Mn2** and HBPin followed by addition of **1**, product **1b** was formed only in trace amount. These observations suggest that the *in situ* activator should be added last, presumably to minimize decomposition of the catalytically active species as well as the semihydrogenation of **1** in the absence of HBPin in case (a) (see below for a mechanistic rationale).

Aiming to increase the yield of **1b**, the reaction conditions were optimized (see Table S5 in the ESI†). The results showed

that conducting the reaction with 10 mol% of catalyst loading, 20 mol% of $NaHBEt_3$ at 30 °C, in a 0.5 M solution of THF and 1.75 equiv. of HBPin for 24 h afforded **1b** in an 86% yield with the reaction proceeding to >99% conversion (catalyst TON = 9 and TOF = 1.3×10^{-4} s^{-1}). Increasing the temperature of the reaction above 30 °C resulted in lower yields for **1b**, presumably due to competition of the semihydrogenation of **1**, as evidenced by the increased amounts of styrene formed as byproduct. Employing other solvents in the reaction such as toluene, acetonitrile or methanol led to decreased yields of **1b** (acetonitrile) or to complete loss of the catalytic activity (toluene and methanol). Preactivation of **Mn2** with 2 equiv. $NaHBEt_3$ also led to a diminished yield for product **1b** (34%), suggesting that the catalytically active species generated upon reaction of **Mn2** with $NaHBEt_3$ might decompose in the absence of the substrates.

The substrate scope for the hydroboration of terminal alkynes catalyzed by **Mn2** was explored under the optimized conditions (see Scheme 2c). **Mn2** was an efficient catalyst for the hydroboration of a moderate number of aromatic and aliphatic alkynes. The yields for the *E*-alkenylboronate esters from hydroboration of phenylacetylene (**1**, 86%, product **1b**) and aromatic alkynes containing electron-donating substituents in the 4-position of the phenyl ring (*e.g.* products **4b** and **6b** with CH_3 and *t*Bu substituents formed in 78% and 89% yields respectively) were high with an excellent chemoselectivity for hydroboration. In contrast, the yield for the *E*-alkenylboronate ester **2b**, obtained when 4-fluorophenylacetylene (**2**) was the substrate, was low (18%), suggesting that electron-withdrawing substituents drastically decrease the efficiency of the catalyst. The position of the substituent in the phenyl ring impacted the efficiency of the catalyst when electron-donating or electron-withdrawing groups were present at the phenyl ring. For example, when the F or CH_3 groups were at the 3-position (substrates **3** and **5** respectively), the yields of products **3b** and **5b** decreased to 10% and 68% respectively, and when these groups were at the 2-position (substrates **9** for and **10** respectively), the *E*-alkenylboronate esters were formed in low yields (6% and <5% for **9b** and **10b** respectively). These results stand in contrast with those observed in the C–H borylation of terminal alkynes employing **Mn1**, where the position of the substituent in the phenyl ring did not impact the efficiency of the catalytic system.[7] The decreased yields as the substituents are closer to the triple bond may be attributed to higher barriers for the insertion steps involved to access *E*-alkenylboronate esters, due to increased steric hindrance between the substrates and the catalytically active species. In line with this hypothesis, the aliphatic alkynes **7** and **8**, containing more flexible alkyl chains, afforded products **7b** and **8b** in higher yields (58% and 66% respectively) than 2-substituted aryl acetylenes.

Mechanistic insights into the hydroboration of terminal alkynes with HBPin catalyzed by $Mn(^{iPr}PNP)Cl_2/NaHBEt_3$

Insights into the reaction pathway. Intrigued by the role of $NaHBEt_3$ in the ability of **Mn2** to increase the chemoselectivity of the reaction, we set out to study the mechanism of this transformation. To interrogate whether there was heterogeneous catalysis involved in the transformation, three Hg drops were added to the catalytic borylation of **1** with HBPin in the presence of 5 mol% of **Mn2** and 10 mol% of $NaHBEt_3$. The catalytic activity was not inhibited and product **1b** formed in a 73% yield, comparable to that when the reaction was run in the absence of Hg (78% yield) and supporting homogenous catalysis operative in the reaction.

To gain insights into the reaction pathway as well as into the identity of the Mn active species, the catalytic hydroboration of 4-fluorophenylacetylene (**2**) with HBPin in the presence of 10 mol% of **Mn2** and 20 mol% of $NaHBEt_3$ employing 1,4-difluorobenzene as internal standard was monitored by ^1H, ^{11}B, ^{31}P and ^{19}F NMR spectroscopy in THF-d_8 at 30 °C for 19 h. An induction period was not observed, and the ^1H and ^{19}F NMR spectra showed the immediate formation of several species at the expense of the starting material (see Scheme 3a for the ^{19}F

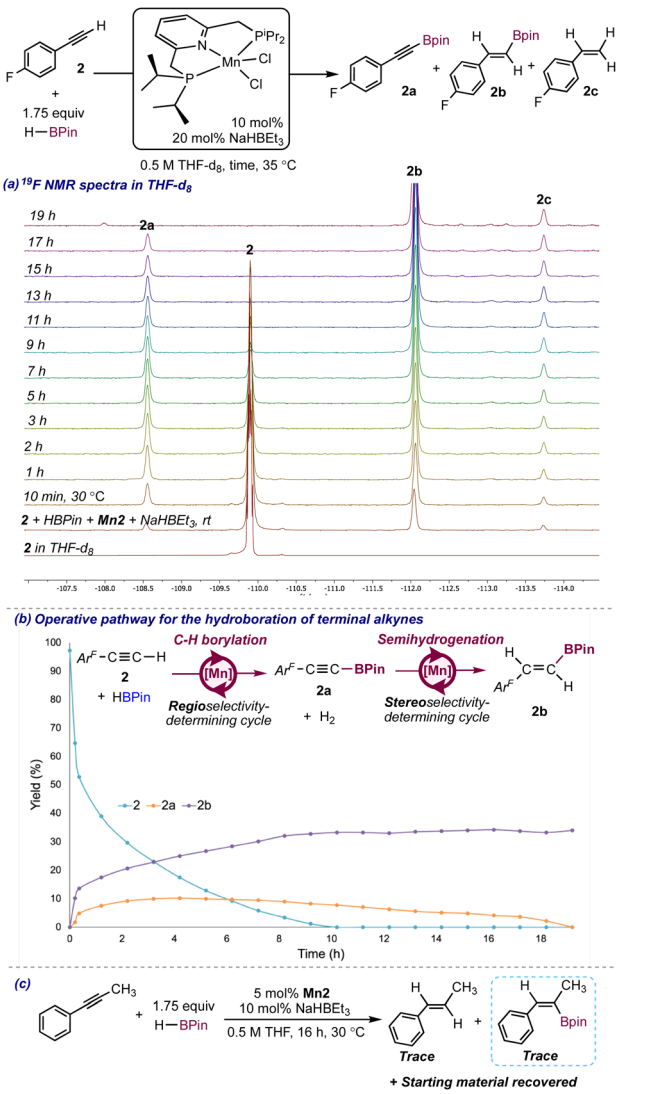

Scheme 3 Mechanistic experiments to gain insights into the reaction pathway, (a) ^{19}F NMR monitoring of the catalytic reaction, (b) proposed reaction pathway and quantitative monitoring of the species during the catalytic reaction and (c) attempted hydroboration of an internal alkyne.

NMR spectra). The major species was identified as the *E*-alkenylboronate ester **2b** whereas the minor species present were (a) the alkynylboronate ester **2a**, (b) 4-fluorophenylethylene (**2c**) and (c) 4-fluorophenylethane (**2d**).

Minor upfield-shifted unidentified signals were also present in the ^{19}F NMR spectra, which can be tentatively attributed to the presence of products from alkyne cyclotrimerization (detected in the crude GC for the hydroboration of **1**) and/or Mn-alkenyl or Mn-alkynyl complexes. The fact that **2a** is present in the reaction medium hints that **Mn2** is efficient for the C(sp)-H borylation of **2**. Consistent with this hypothesis, H_2 was observed (singlet at 4.55 ppm) in the ^{1}H NMR spectra. The presence of **2c** in the reaction medium supports that **Mn2** is also efficient for the semihydrogenation of **2**, which is consistent with previous reports describing **Mn2** as an efficient catalyst for the *Z*-stereoselective transfer semihydrogenation of internal alkynes.[10] The starting material was consumed in 10 hours, however, the **2a** : **2b** ratio changed after full conversion (Scheme 3b). The changes in the yields of **2a** and **2b** over time supported that **2b** formed at the expense of **2a**, with this conversion being complete in 19 h, time after which the amounts of all the species in solution remained constant. The ^{1}H NMR spectra showed the formation of H_2 followed by its gradual consumption as **2b** was forming at the expense of **2a** (see Fig. S8 in the ESI†). These observations point toward a reaction pathway involving tandem C–H borylation/semihydrogenation to access **2b** with the C–H borylation cycle being the regioselectivity-determining and the semihydrogenation cycle the stereoselectivity-determining (Scheme 3b). Because both, **2a** and **2b**, are present at the initial stages of the reaction, exclusive formation of **2b** by stereo- and regioselective hydroboration of **2** may also be operative. Interestingly, **Mn2**/$NaHBEt_3$ is *E*-stereoselective for the semihydrogenation of **2a**, which stands in contrast to the reported *Z* stereoselectivity for the semihydrogenation of internal alkynes with NH_3BH_3 catalyzed by **Mn2**,[10] suggesting that the identity of the substrate (internal alkyl or aryl alkyne *vs.* alkynylboronate ester) and/or the identity of the activator (NH_3BH_3 *vs.* $NaHBEt_3$) play a relevant role in the stereoselectivity of the semihydrogenation reaction.

Because 4-fluorophenylstyrene (**2c**) is also formed as a byproduct, at least three catalytic cycles are operative in the reaction medium: (a) one for the semihydrogenation of **2**, (b) one for the C–H borylation of **2**, and (c) one for the semihydrogenation of **2a**, with cycles (b) and (c) being responsible for the formation of **2b**. The ^{31}P NMR spectra showed signals for 3 P-containing species (at 0.60 (major), −0.50 (minor) and −2.18 ppm (minor), see bottom spectrum in Scheme 4e) which did not correspond to free ^{iPr}PNP ligand, neither to putative products from the reaction of the free ^{iPr}PNP ligand with HBPin and can be tentatively assigned to catalyst resting-states. The signal at −0.50 ppm disappeared after 2 h of reaction, whereas the those at 0.60 and −2.18 ppm remained intact during catalytic turnover, pointing toward these species as the catalyst resting-states for the C–H borylation and semihydrogenation cycles responsible for the formation of **2b**. Furthermore, both signals appeared at different chemical shifts than those for the catalyst resting-states when **Mn2** was employed in the absence of $NaHBEt_3$ (38.0 and 38.5 ppm, see Fig. S5 in the ESI†), supporting different catalyst

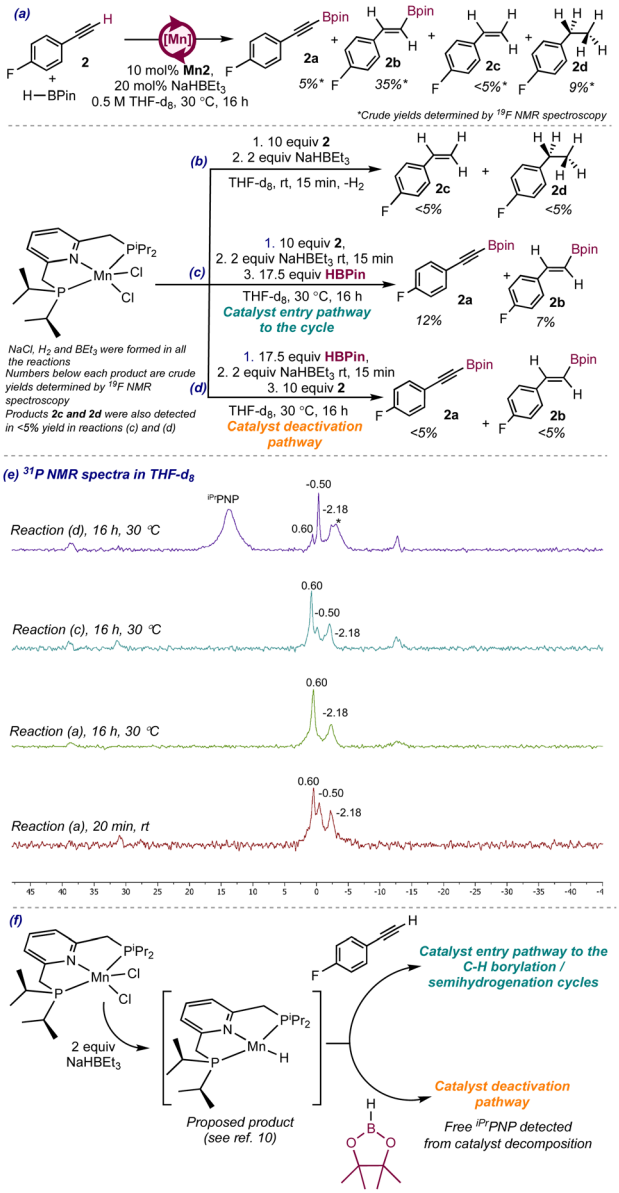

Scheme 4 (a) Product yields in the catalytic reaction after 16 h. Mechanistic experiments to gain insights into precatalyst entry pathway to the cycle: (b) addition of $NaHBEt_3$ to a mixture of **Mn2** and excess **2**; (c) addition of $NaHBEt_3$ to a mixture of **Mn2** and excess **2** followed by addition of excess HBPin and (d) addition of $NaHBEt_3$ to a mixture of **Mn2** and excess HBPin followed by addition of excess **2**. (e) Stacked ^{31}P NMR spectra in THF-d_8 for the catalytic reaction (a) and reactions (c) and (d); (f) proposed catalyst entry to the cycle and deactivation pathway. Chemical shifts are reported in ppm close to each signal. * denotes an unidentified signal at −3.13 ppm.

resting-states when the reaction is conducted in the presence of $NaHBEt_3$. Signals attributable to diamagnetic Mn species were not identified in the ^{1}H NMR spectra of the reaction, presumably obscured by the signals of **2**, **2a**, **2b** and **2c**.

Further supporting a tandem C–H borylation/semihydrogenation pathway operative in catalysis, the hydroboration of the internal alkyne 1-phenyl-1-propyne catalyzed by **Mn2**/$NaHBEt_3$ proceeded to low conversion with the corresponding *E*-alkenylboronate ester and alkene detected in trace

amounts in the reaction crude (by ^{1}H NMR spectroscopy and GC, see Scheme 3c). Because this substrate lacks C(sp)–H groups, a C–H borylation/semihydrogenation pathway is not accessible, and only a hydroboration cycle involving alkyne insertion and C(sp^2)–B formation steps can be operative to yield the alkenylboronate ester. However, this cycle may be inaccessible due to high energy barriers resulting in no catalytic activity for this process.

Although catalysts capable of performing tandem C–H borylation/hydroboration are known,[13] the potential of manganese catalysts in tandem processes, which is still the realm of precious metals,[14] is underexploited. Therefore, the results reported here constitute a first step toward the design of manganese catalysts efficient for tandem transformations.

Insights into the precatalyst entry to the cycle for the hydroboration of alkynes catalyzed by Mn2/NaHBEt$_3$. To gain insights into the precatalyst entry pathway to the cycle, 2 equivalents of $NaHBEt_3$ were added to a THF solution of **Mn2** at −78 °C. The ^{1}H and ^{31}P of the reaction crude in C_6D_6 showed signals attributable to free ^{iPr}PNP ligand, hinting decomposition of the product. Previous work has supported the formation of a catalytically active Mn(I)–H by DFT calculations in the semihydrogenation of internal alkynes catalyzed by **Mn2** with NH_3BH_3 as *in situ* activator.[10] If the same catalytically active species was formed upon activation with $NaHBEt_3$, its electronic unsaturation (14 electrons) could lead to decomposition in the absence of substrates. This is consistent with the observation that preactivation of **Mn2** with $NaHBEt_3$ lead to a lower yield of the *E*-alkenylboronate ester **1b** in the catalytic hydroboration of **1** (see above). Aiming to stabilize the putative Mn–H complex, the addition of 2 equiv. of $NaHBEt_3$ to **Mn2** was conducted in the presence of 2 equivalents of 2-electron donor ligands such as PMe_3, *t*BuCN or 2,6-$Me_2C_5H_4CN$. In all cases the efforts to isolate and characterize a manganese complex failed, and only when *t*BuCN was employed, a signal consistent with the presence of a hydride ligand (at −4.53 ppm, *t*, $^2J_{HP}$ = 49.2 Hz) in a diamagnetic {Mn(PNP)} complex[15] could be detected in the reaction crude by ^{1}H NMR spectroscopy (see Fig. S14 in the ESI†). Further work is ongoing in our laboratory to isolate and fully characterize this complex.

To identify whether the putative Mn–H enters the cycle by reaction with the alkyne, the reaction of **Mn2** with 2 equiv. of $NaHBEt_3$ in the presence of 10 equivalents of **2** was conducted in THF-d_8 in a J. Young NMR tube at room temperature in the presence of 1,4-difluorobenzene as internal standard and the ^{1}H, ^{19}F and ^{31}P NMR spectra were registered (see second ^{19}F and ^{1}H NMR spectra from the bottom in Fig. S16–S19† and bottom ^{31}P NMR spectrum in Fig. S21 in the ESI† and Scheme 4b). Immediately after the addition of $NaHBEt_3$ to the mixture of **Mn2** and **2**, the ^{19}F NMR spectra showed signals consistent with the presence of **2c** (−113.4 ppm) and 4-fluorophenylethane (−117.0 ppm) (see second from the bottom^{19}F NMR spectrum in Fig. S16 in the ESI†), formed by hydrogenation of **2** (−109.4 ppm). Accordingly, the ^{1}H NMR spectra hinted the presence of H_2 (at 4.50 ppm, see second ^{1}H NMR spectrum from the bottom in Fig. S18†). As in the monitoring of the catalytic reaction, minor upfield shifted signals in the ^{19}F NMR spectra may hint the presence of Mn-alkenyl or Mn-alkynyl complexes and of products from alkyne cyclotrimerization. The ^{31}P NMR spectra did not show any signal attributable to diamagnetic Mn complexes neither to free ^{iPr}PNP (see bottom ^{31}P NMR spectrum in Fig. S21 in the ESI†). These results suggest that, in the absence of HBPin, **Mn2** can catalyze the semihydrogenation of **2** to **2c** and the full hydrogenation to **2d** with the H_2 generated from precatalyst activation and allow to rationalize the presence of **2c** and **2d** as byproducts in the hydroboration of **2**.

Addition of excess HBPin to the reaction mixture resulted in the immediate formation of **2a** (−108.0 ppm) and **2b** (−111.5 ppm) (see Fig. S16 in the ESI†). This result supports reaction of the putative Mn–H active species with the alkyne **2** as the catalyst entry pathway to the cycle (Scheme 4f). Therefore, the active Mn–H would activate the C–H bond of **2** to yield **2a** in a first C–H borylation cycle followed by insertion of the triple bond of **2a** in a second semihydrogenation cycle that would yield **2b**. The ^{31}P NMR spectra showed the presence of 3 species at 0.60 (major), −0.50 (minor) and −2.18 ppm (minor), consistent with diamagnetic Mn complexes present in the reaction medium (see spectrum for reaction (c) after 16 h in Scheme 4e). More importantly, the species at 0.60 and −2.18 ppm were also present in the ^{31}P NMR spectra of the catalytic reaction (see spectrum for reaction (a) after 16 h in Scheme 4e), which supports them as the catalyst resting-states for the C–H borylation and semihydrogenation cycles responsible for the formation of **2b**, and the reaction of the Mn–H with the alkyne as the catalyst entry pathway to the C–H borylation cycle. Attempts to isolate or characterize a Mn complex from the reaction of **Mn2** with 2 equiv. of $NaHBEt_3$ in the presence of 3 equivalents of **2** failed and the crude ^{1}H and ^{19}F NMR spectra showed peaks consistent with the presence of **2c** and **2d**, suggesting that the *in situ* generated Mn–H catalyzed the hydrogenation of **2**.

The results presented above support that, when only H_2 is present in the reaction medium after precatalyst activation, the C–H bond activation pathway is unproductive and the insertion pathways yielding **2c** and **2d** are preferred. However, in the presence of HBPin, the tandem C–H borylation/semihydrogenation catalytic cycles are preferred, accounting for the formation of the major product **2b**. Because the amount of **2c** increases over time even in the presence of HBPin but to a lower extent than the amounts of **2b** and **2a**, the semihydrogenation of **2** is still operative in the presence of HBPin, however, it is slower than the tandem C–H borylation/semihydrogenation that yields **2b**.

Aiming to identify other catalytically active species, the reaction of **Mn2** with 2 equiv. of $NaHBEt_3$ in the presence of 10 equivalents of HBPin was conducted in THF-d_8 in a J. Young NMR tube and the ^{1}H, ^{11}B and the ^{31}P NMR spectra were registered at room temperature (see Fig. S22–S26 in the ESI†). The ^{1}H and ^{11}B NMR spectra only showed signals attributable to HBPin, however, the ^{31}P showed two signals, at 13.4 ppm (major), attributable to free ^{iPr}PNP ligand, and at −0.50 ppm (minor) (see bottom ^{31}P NMR spectrum in Fig. S26 in the ESI†), which also appeared as a minor species at early stages of the catalytic reaction and when HBPin was added to a mixture of

Mn2, **2** and $NaHBEt_3$ (see spectrum for reaction (c) after 16 h in Scheme 4e). The presence of free ^{iPr}PNP ligand in the reaction crude points toward partial decomposition of the manganese complex formed upon reaction of **Mn2** with HBPin and $NaHBEt_3$.

Addition of excess **2** to the reaction mixture resulted in the formation of products **2a**, **2b** and **2c** (see ^{19}F NMR monitoring in Fig. S22 of the ESI†), suggesting catalytic turnover taking place after addition of **2**. However, the reaction only proceeded to 18% conversion after 16 hours, significantly lower than the conversion for the catalytic reaction (98% after 16 hours), and than when HBPin was added to a mixture of **Mn2**, $NaHBEt_3$ and **2** (64% after 16 hours). This result points to the reaction of the putative Mn–H with HBPin as a catalyst deactivation pathway (Scheme 4f), consistent with the presence of free ^{iPr}PNP ligand in the ^{31}P NMR spectra, and allows to rationalize why the order of addition of the reagents in the catalytic reaction impacted the yield of product **1b**. When $NaHBEt_3$ was added to a mixture of HBPin and **Mn2** followed by addition of **1** (see above), trace amount of **1b** was observed due to deactivation of the catalytically active Mn–H by HBPin before the addition of **1**. The presence of this deactivation pathway in the catalytic reaction prevents the recyclability of the catalyst and limits its lifetime to 19 h for the hydroboration of **2**. Alternatively, when $NaHBEt_3$ was added to a mixture of **1** and **Mn2** followed by the addition of HBPin, the catalytic reaction proceeded as the Mn–H entered the first catalytic cycle by reaction with **1**. However, in this instance **1b** was formed in lower yield (44%) than when $NaHBEt_3$ was added to a mixture of **Mn2**, HBPin and **1** (78%), which could be attributed to partial decomposition of the active species formed upon reaction of the Mn–H with **1** before the addition of HBPin.

Additionally, the ^{31}P NMR spectra showed the presence of the signals at 0.60, −0.50 and −2.18 ppm (see top spectrum in Scheme 4e), consistent with the presence of catalytically active species that would be responsible for the formation of products **2a**, **2b** and **2c**. However, because the species formed after reaction of **Mn2**/$NaHBEt_3$ with HBPin decomposed to a large extent as evidenced by the presence of free ^{iPr}PNP ligand as the major product, the concentration of the catalytically active species is presumed to be low, resulting in a low conversion of the starting material and low yields of the products.

Further mechanistic studies are currently undergoing in our laboratory aiming to elucidate the identity of the catalytically active species.

Conclusions

In summary, we have discovered the first manganese catalyst for the hydroboration of terminal alkynes. The presence of $NaHBEt_3$ as precatalyst activator was found to enhance the chemoselectivity of the process and the efficiency of the catalytic system. Aromatic alkynes with electron-donating groups at the phenyl rings and aliphatic alkynes, mainly 1-octene and 3-methyl-1-butyne, were hydroborated with an excellent chemo-, regio- and stereoselectivity. In contrast, when electron-withdrawing substituents were present in the phenyl ring the catalytic activity plummeted. In all the cases, the position of the substituent in the phenyl ring (2 *vs.* 3 *vs.* 4) impacted the efficiency of the system, with 2-substituted aryl alkynes leading to the loss of the catalytic activity. The hydroboration reaction was found to proceed by a tandem C–H borylation/*E*-stereoselective semihydrogenation pathway, with the C–H borylation step resulting on β-regioselectivity and the semihydrogenation step affording exclusively the *E*-alkenylboronate ester. Stoichiometric reactions support that the precatalyst entered the cycle by reaction with $NaHBEt_3$ followed by reaction with the alkyne, whereas reaction with HBPin led to decomposition of the Mn complex and constituted a catalyst deactivation pathway. Further mechanistic studies are currently being carried out in our laboratory to elucidate the identity of the Mn species involved in the catalytic cycles.

Author contributions

R. A. designed the experiments, supervised the experimental work and drafted the manuscript. V. D. A. designed the experiments, conducted the experimental work and drafted the ESI.† The manuscript was written through contributions of all authors. All authors have given approval to the final version of the manuscript.

Conflicts of interest

There are no conflicts to declare.

Acknowledgements

R. A. acknowledges the NSF for a LEAPS-MPS grant (# 2316526) and UC Merced for start-up funds. R. A. and V. D. A. thank Himani Ahuja for a generous gift of HBDan.

Notes and references

1 (*a*) J. Jiao and Y. Nishihara, Alkynylboron Compounds in Organic Synthesis, *J. Organomet. Chem.*, 2012, 3–16; (*b*) S. Nandy, S. Paul, K. K. Das, P. Kumar, D. Ghorai and S. Panda, Synthesis and reactivity of alkynyl boron compounds, *Org. Biomol. Chem.*, 2021, **19**, 7276–7297; (*c*) J. Carreras, A. Caballero and P. J. Perez, Alkenyl Boronates: Synthesis and Applications, *Chem.–Asian J.*, 2019, **14**, 329–343; (*d*) J. El-Maiss, T. M. El Dine, C.-S. Lu, I. Karame, A. Kanj, K. Polychronopoulou and J. Shaya, Recent advances in metal-catalyzed alkyl-boron (C(sp3)-C(sp2)) Suzuki-Miyaura cross-couplings, *Catalysts*, 2020, **10**, 296; (*e*) W. N. Palmer, C. Zarate and P. J. Chirik, Benzyltriboronates: Building Blocks for Diastereoselective Carbon–Carbon Bond Formation, *J. Am. Chem. Soc.*, 2017, **139**, 2589–2592.

2 (*a*) S. J. Geier, C. M. Vogels, J. A. Melanson and S. A. Westcott, The transition metal-catalysed hydroboration reaction, *Chem. Soc. Rev.*, 2022, **51**, 8877–8922; (*b*) A. Singh, S. Shafiei-Haghighi, C. R. Smith, D. K. Unruh and M. Findlater, Hydroboration of Alkenes and Alkynes

Employing Earth-Abundant Metal Catalysts, *Asian J. Org. Chem.*, 2020, **9**, 416–420; (*c*) E. A. Romero, R. Jazzar and G. Bertrand, (CAAC)CuX-catalyzed hydroboration of terminal alkynes with pinacolborane directed by the X-ligand, *J. Organomet. Chem.*, 2017, **829**, 11e13; (*d*) K. Jaiswal, K. Groutchik, D. Bawari and R. Dobrovetsky, An "On-Demand", Selective Dehydrogenative Borylation or Hydroboration of Terminal Alkynes Using Zn^{2+}-based Catalyst, *ChemCatChem*, 2022, **14**, e202200004; (*e*) S. Weber, D. Zobernig, B. Stöger, L. F. Veiros and K. Kirchner, Hydroboration of Terminal Alkenes and trans-1,2-Diboration of Terminal Alkynes Catalyzed by a Manganese(I) Alkyl Complex, *Angew. Chem., Int. Ed.*, 2021, **60**, 24488–24492; (*f*) N. Gorgas, L. G. Alves, B. Stöger, A. M. Martins, L. F. Veiros and K. Kirchner, Stable, Yet Highly Reactive Nonclassical Iron(II) Polyhydride Pincer Complexes: Z-Selective Dimerization and Hydroboration of Terminal Alkynes, *J. Am. Chem. Soc.*, 2017, **139**, 8130–8133; (*g*) J. V. Obligacion, J. M. Neely, A. N. Yazdani, I. Pappas and P. J. Chirik, Cobalt Catalyzed Z-Selective Hydroboration of Terminal Alkynes and Elucidation of the Origin of Selectivity, *J. Am. Chem. Soc.*, 2015, **137**, 5855–5858; (*h*) S. Mandal, S. Mandal and K. Geetharani, Zinc-Catalysed Hydroboration of Terminal and Internal Alkynes, *Chem.–Asian J.*, 2019, **14**, 4553–4556; (*i*) H. Ben-Daat, C. L. Rock, M. Flores, T. L. Groy, A. C. Bowman and R. J. Trovitch, Hydroboration of alkynes and nitriles using an a-diimine cobalt hydride catalyst, *Chem. Commun.*, 2017, **53**, 7333–7336; (*j*) J. Chen, X. Shen and Z. Lu, Cobalt-Catalyzed Markovnikov-Type Selective Hydroboration of Terminal Alkynes, *Angew. Chem., Int. Ed.*, 2021, **60**, 690–694; (*k*) C. K. Blasius, V. Vasilenko, R. Matveeva, H. Wadepohl and L. H. Gade, Reaction Pathways and Redox States in a-Selective Cobalt-Catalyzed Hydroborations of Alkynes, *Angew. Chem., Int. Ed.*, 2020, **59**, 23010–23014; (*l*) K. Nakajima, T. Kato and Y. Nishibayashi, Hydroboration of Alkynes Catalyzed by Pyrrolide-Based PNP Pincer−Iron Complexes, *Org. Lett.*, 2017, **19**, 4323–4326; (*m*) W. J. Jang, W. L. Lee, J. H. Moon, J. Y. Lee and J. Yun, Copper-Catalyzed trans-Hydroboration of Terminal Aryl Alkynes: Stereodivergent Synthesis of Alkenylboron Compounds, *Org. Lett.*, 2016, **18**, 1390–1393; (*n*) M. J. González, F. Bauer and B. Breit, Cobalt-Catalyzed Hydroboration of Terminal and Internal Alkynes, *Org. Lett.*, 2021, **23**, 8199–8203; (*o*) S. Garhwal, N. Fridman and G. de Ruiter, Z-Selective Alkyne Functionalization Catalyzed by a trans-Dihydride N-Heterocyclic Carbene (NHC) Iron Complex, *Inorg. Chem.*, 2020, **59**, 13817–13821; (*p*) H. Yoshida, Borylation of Alkynes underBase/Coinage Metal Catalysis: Some Recent Developments, *ACS Catal.*, 2016, **6**, 1799–1811; (*q*) K. Yamamoto, Y. Mohara, Y. Mutoh and S. Saito, Ruthenium-Catalyzed (Z)-Selective Hydroboration of Terminal Alkynes with Naphthalene-1,8-diaminatoborane, *J. Am. Chem. Soc.*, 2019, **141**, 17042–17047; (*r*) C. Gunanathan, M. Hölscher, F. Pan and W. Leitner, Ruthenium Catalyzed Hydroboration of Terminal Alkynes to Z-Vinylboronates, *J. Am. Chem. Soc.*, 2012, **134**, 14349–14352; (*s*) A. L. Narro, H. D. Arman and Z. J. Tonzetich, Mechanistic Studies of Alkyne Hydroboration by a Well-Defined Iron Pincer Complex: Direct Comparison of Metal-Hydride and Metal-Boryl Reactivity, *Inorg. Chem.*, 2022, **61**, 10477–10485.

3 (*a*) C.-I. Lee, J. Zhou and O. V. Ozerov, Catalytic dehydrogenative borylation of terminal alkynes by a SiNN pincer complex of iridium, *J. Am. Chem. Soc.*, 2013, **135**, 3560–3566; (*b*) B. J. Foley, N. Bhuvanesh, J. Zhou and O. V. Ozerov, Combined Experimental and Computational Studies of the Mechanism of Dehydrogenative Borylation of Terminal Alkynes Catalyzed by PNP Complexes of Iridium, *ACS Catal.*, 2020, **10**, 9824–9836; (*c*) B. J. Foley and O. V. Ozerov, Air- and Water-Tolerant (PNP)Ir Precatalyst for the Dehydrogenative Borylation of Terminal Alkynes, *Organometallics*, 2020, **39**, 2352–2355; (*d*) E. A. Romero, R. Jazzar and G. Bertrand, Copper-catalyzed dehydrogenative borylation of terminal alkynes with pinacolborane, *Chem. Sci.*, 2017, **8**, 165–168; (*e*) R. J. Procter, M. Uzelac, J. Cid, P. J. Rushworth and M. J. Ingleson, Low-Coordinate NHC-Zinc Hydride Complexes Catalyze Alkyne C-H Borylation and Hydroboration Using Pinacolborane, *ACS Catal.*, 2019, **9**, 5760–5771; (*f*) D. Lewandowski, T. Cytlak, R. Kempe and G. Hreczycho, Ligand-controlled Cobalt-Catalyzed formation of Carbon-Boron bonds: Hydroboration *vs.* C-H/B-H dehydrocoupling, *J. Catal.*, 2022, **413**, 728–734; (*g*) C. J. Pell and O. V. Ozerov, Catalytic dehydrogenative borylation of terminal alkynes by POCOP-supported palladium complexes, *Inorg. Chem. Front.*, 2015, **2**, 720–724; (*h*) T. Tsuchimoto, H. Utsugi, T. Sugiura and S. Horio, Alkynylboranes: A Practical Approach by Zinc-Catalyzed Dehydrogenative Coupling of Terminal Alkynes with 1,8-Naphthalenediaminatoborane, *Adv. Synth. Catal.*, 2015, **357**, 77–82; (*i*) D. Wei, B. Carboni, B. J.-B. Sortais and C. Darcel, Iron-Catalyzed Dehydrogenative Borylation of Terminal Alkynes, *Adv. Synth. Catal.*, 2018, **360**, 3649–3654; (*j*) J.-R. Hu, L.-H. Liu, X. Hu and H.-D. Ye, Ag(I)-catalyzed C-H borylation of terminal alkynes, *Tetrahedron*, 2014, **70**, 5815–5819; (*k*) M. Luo, Y. Qin, X. Chen, Q. Xiao, B. Zhao, W. Yao and M. Ma, $ZnBr_2$-Catalyzed Dehydrogenative Borylation of Terminal Alkynes, *J. Org. Chem.*, 2021, **86**, 16666–16674.

4 (*a*) M. Haberberger and S. Enthaler, Straightforward Iron-Catalyzed Synthesis of Vinylboronates by the Hydroboration of Alkynes, *Chem.–Asian J.*, 2013, **8**, 50–54; (*b*) L. Ferrand, Y. Lyu, A. Rivera-Hernández, B. J. Fallon, M. Amatore, C. Aubert and M. Petit, Hydroboration and Diboration of Internal Alkynes Catalyzed by a Well-Defined Low-Valent Cobalt Catalyst, *Synth*, 2017, **49**, 3895–3904; (*c*) F. Rami, F. Bächtle and B. Plietker, Hydroboration of internal alkynes catalyzed by Fe(CO)(NO)(PPh3)2: a case of boron-source controlled regioselectivity, *Catal. Sci. Technol.*, 2020, **10**, 1492–1497; (*d*) G. Zhang, H. Zeng, S. Zheng, M. C. Neary and P. A. Dub, Vanadium-Catalyzed Stereo- and Regioselective Hydroboration of Alkynes to Vinyl Boronates, *ACS Catal.*, 2022, **12**, 5425–5429.

5 (*a*) K. Das, M. K. Barman and B. Maji, Advancements in multifunctional manganese complexes for catalytic hydrogen transfer reactions, *Chem. Commun.*, 2021, **57**, 8534–8549 and references therein;; (*b*) K. Das, S. Waiba, A. Jana and B. Maji, Manganese-catalyzed hydrogenation, dehydrogenation, and hydroelementation reactions, *Chem. Soc. Rev.*, 2022, **51**, 4386–4464 and references therein;; (*c*) E. S. Gulyaeva, E. S. Osipova, R. Buhaibeh, Y. Canac, J. B. Sortais and D. A. Valyaev, Towards ligand simplification in manganese-catalyzed hydrogenation and hydrosilylation processes, *Coord. Chem. Rev.*, 2022, **458**, 214421; (*d*) P. Schlichter and C. Werle, The Rise of Manganese-Catalyzed Reduction Reactions, *Synth*, 2022, **54**, 517–534; (*e*) A. Torres-Calis and J. J. García, Homogeneous Manganese-Catalyzed Hydrofunctionalizations of Alkenes and Alkynes: Catalytic and Mechanistic Tendencies, *ACS Omega*, 2022, **7**, 37008–37038; (*f*) D. M. Sharma, A. B. Shabade, R. G. Gonnade and B. Punji, Manganese(I)-Catalyzed Chemoselective Transfer Hydrogenation of the C=C Bond in Conjugated Ketones at Room Temperature, *Chem.–Eur. J.*, 2023, **29**, e202301174; (*g*) R. A. Farrar-Tobar, S. Weber, Z. Csendes, A. Ammaturo, S. Fleissner, H. Hoffmann, L. F. Veiros and K. Kirchner, E-Selective Manganese-Catalyzed Semihydrogenation of Alkynes with H2 Directly Employed or *In Situ*-Generated, *ACS Catal.*, 2022, **12**, 2253–2260.

6 (*a*) Y. P. Zhou, Z. Mo, M. P. Luecke and M. Driess, Stereoselective Transfer Semi-Hydrogenation of Alkynes to E-Olefins with N-Heterocyclic Silylene-Manganese Catalysts, *Chem.–Eur. J.*, 2018, **24**, 4780–4784; (*b*) R. J. Trovitch, The Emergence of Manganese-Based Carbonyl Hydrosilylation Catalysts, *Acc. Chem. Res.*, 2017, **50**, 2842–2852; (*c*) T. K. Mukhopadhyay, M. Flores, T. L. Groy and R. J. Trovitch, A Highly Active Manganese Precatalyst for the Hydrosilylation of Ketones and Esters, *J. Am. Chem. Soc.*, 2014, **136**, 882–885; (*d*) T. K. Mukhopadhyay, M. Flores, T. L. Groy and R. J. Trovitch, A β-diketiminate manganese catalyst for alkene hydrosilylation: substrate scope, silicone preparation, and mechanistic insight, *Chem. Sci.*, 2018, **9**, 7673–7680; (*e*) G. Zhang, H. Zeng, J. Wu, Z. Yin, S. Zheng and J. C. Fettinger, Highly Selective Hydroboration of Alkenes, Ketones and Aldehydes Catalyzed by a Well-Defined Manganese Complex, *Angew. Chem.*, 2016, **128**, 14581–14584; (*f*) L. Britton, M. Krodzki, G. S. Nichol, A. P. Dominey, P. Pawluc, J. H. Docherty and S. P. Thomas, Manganese-Catalyzed C(sp2)-H Borylation of Furan and Thiophene Derivatives, *ACS Catal.*, 2021, **11**, 6857–6864.

7 H. Ahuja, H. Kaur and R. Arevalo, Chemoselective C(sp)–H borylation of terminal alkynes catalyzed by a bis(N-heterocyclicsilylene) manganese complex, *Inorg. Chem. Front.*, 2023, **10**, 6067–6076.

8 A. Brzozowska, V. Zubar, R.-C. Ganardi and M. Rueping, Chemoselective Hydroboration of Propargylic Alcohols and Amines Using a Manganese(II) Catalyst, *Org. Lett.*, 2020, **22**, 3765–3769.

9 (*a*) S. Kalra, D. Pividori, D. Fehn, C. Dai, S. Dong, S. Yao, J. Zhu, K. Meyer and M. Driess, A bis(silylene)pyridine pincer ligand can stabilize mononuclear manganese(0) complexes: facile access to isolable analogues of the elusive d7-Mn(CO)5 radical, *Chem. Sci.*, 2022, **13**, 8634–8641; (*b*) H. Ren, Y.-P. Zhou, Y. Bai, C. Cui and M. Driess, Cobalt-Catalyzed Regioselective Borylation of Arenes: N-Heterocyclic Silylene as an Electron Donor in the Metal-Mediated Activation of C−H Bonds, *Chem.–Eur. J.*, 2017, **23**, 5663–5667; (*c*) R. Arevalo, T. P. Pabst and P. J. Chirik, C(sp2)-H Borylation of Heterocycles by Well-Defined Bis(silylene)pyridine Cobalt(III) Precatalysts: Pincer Modifica-tion, C(sp2)-H Activation, and Catalytically Relevant Intermedi-ates, *Organometallics*, 2020, **39**, 2763–2773; (*d*) Y. P. Zhou and M. Driess, Isolable Silylene Ligands Can Boost Efficiencies and Selectivities in Metal-Mediated Catalysis, *Angew. Chem., Int. Ed.*, 2019, **58**, 3715–3728; (*e*) D. Gallego, S. Inoue, B. Blom and M. Driess, Highly Electron-Rich Pincer-Type Iron Complexes Bearing Innocent Bis(metallylene)pyridine Ligands: Syntheses, Structures, and Catalytic Activity, *Organometallics*, 2014, **33**, 6885–6897.

10 A. Brzozowska, L. M. Azofra, V. Zubar, I. Atodiresei, L. Cavallo, M. Rueping and O. El-Sepelgy, Highly Chemo- and Stereoselective Transfer Semihydrogenation of Alkynes Catalyzed by a Stable, Well-Defined Manganese(II) Complex, *ACS Catal.*, 2018, **8**, 4103–4109.

11 S. Arepally, P. Nandhakumar, G. A. González-Montiel, A. Dzhaparova, G. Kim, A. Ma, K. M. Nam, H. Yang, P. H.-Y. Cheong and J. K. Park, Unified Electrochemical Synthetic Strategy for [2 + 2 + 2] Cyclotrimerizations: Construction of 1,3,5- and 1,2,4-Trisubstituted Benzenes from Ni(I)-Mediated Reduction of Alkynes, *ACS Catal.*, 2022, **12**, 6874–6886.

12 A. D. Bage, T. A. Hunt and S. P. Thomas, Hidden Boron Catalysis: Nucleophile-Promoted Decomposition of HBpin, *Org. Lett.*, 2020, **22**, 4107–4112.

13 (*a*) Q. Lai and O. V. Ozerov, Dehydrogenative Diboration of Alkynes Catalyzed by Ir/CO/tBuNC System, *J. Organomet. Chem.*, 2021, **931**, 121614; (*b*) Y. Gao, Z. Q. Wu and K. M. Engle, Synthesis of Stereodefined 1,1-Diborylalkenes *via* Copper-Catalyzed Di-boration of Terminal Alkynes, *Org. Lett.*, 2020, **22**, 5235–5239; (*c*) S. Krautwald, M. J. Bezdek and P. J. Chirik, Cobalt-Catalyzed 1,1-Diboration of Terminal Alkynes: Scope, Mechanism, and Synthetic Applications, *J. Am. Chem. Soc.*, 2017, **139**, 3868–3875; (*d*) C. I. Lee, W. C. Shih, J. Zhou, J. H. Reibenspies and O. V. Ozerov, Synthesis of Triborylalkenes from Terminal Alkynes by Iridium-Catalyzed Tandem C-H Borylation and Diboration, *Angew. Chem., Int. Ed.*, 2015, **54**, 14003–14007; (*e*) X. Liu, W. Ming, Y. Zhang, A. Friedrich and T. B. Marder, Copper-Catalyzed Triboration: Straightforward, Atom-Economical Synthesis of 1,1,1-Triborylalkanes from Terminal Alkynes and HBpin, *Angew. Chem., Int. Ed.*, 2019, **58**, 18923–18927.

14 (*a*) R. T. Ruck, M. A. Huffman, M. M. Kim, M. Shevlin, W. V. Kandur and I. W. Davies, Palladium-Catalyzed

Tandem Heck Reaction/C-H Functionalization—Preparation of Spiro-Indane-Oxindoles, *Angew. Chem., Int. Ed.*, 2008, **47**, 4711–4714; (*b*) S. S. Ichake, A. Konala, V. Kavala, C.-W. Kuo and C.-F. Yao, Palladium-Catalyzed Tandem C−H Functionalization/Cyclization Strategy for the Synthesis of 5-Hydroxybenzofuran Derivatives, *Org. Lett.*, 2017, **19**, 54–57; (*c*) M. K. Armstrong, M. B. Goodstein and G. Lalic, Diastereodivergent Reductive Cross Coupling of Alkynes throughTandem Catalysis: Z- and E-Selective Hydroarylation of Terminal Alkynes, *J. Am. Chem. Soc.*, 2018, **140**, 10233–10241; (*d*) J.-C. Wasilke, S. J. Obrey, R. T. Baker and G. C. Bazan, Concurrent Tandem Catalysis, *Chem. Rev.*, 2005, **105**, 1001–1020; (*e*) Y. You and S. Ge, Cobalt-Catalyzed One-Pot Asymmetric Difunctionalization of Alkynes to Access Chiral gem-(Borylsilyl)alkanes, *Angew. Chem., Int. Ed.*, 2021, **60**, 20684–20688.

15 M. Glatz, B. Stoeger, D. Himmelbauer, L. F. Veiros and K. Kirchner, Chemoselective Hydrogenation of Aldehydes under Mild, Base-Free Conditions: Manganese Outperforms Rhenium, *ACS Catal.*, 2018, **8**, 4009–4016.